DMD Fast Forward. Published on May 12, 2006 as doi:10.1124/dmd.105.009027

DMD #9027

Species Differences in Metabolism and Pharmacokinetics of a Sphingosine-1-Phosphate Receptor Agonist in Rats and Dogs: Formation of a Unique Glutathione Adduct in the Rat

M. Reza Anari, Mellissa D. Creighton, Jason S. Ngui, Richard A. Tschirret-Guth, Yohannes Teffera, George A. Doss, Wei Tang, Nathan X. Yu, Suzanne L. Ciccotto, Donald F. Hobra Jr., John B. Coleman, Stella H. Vincent and David C. Evans

Department of Drug Metabolism (M.R.A. [1]) and Department of Safety Assessment (J.B.C.), Merck Research Labs, West Point, Pennsylvania; Department of Drug Metabolism (M.D.C., J.S.N., R.A.T., Y.T. [2], G.A.D., W.T., N.X.Y., S.L.C., S.H.V., D.C.E.[3]) and Department of Comparative Medicine (D.H. Jr.), Merck Research Labs Rahway, New Jersey

DMD Fast Forward. Published on May 12, 2006 as DOI: 10.1124/dmd.105.009027
This article has not been copyedited and formatted. The final version may differ from this version.

Running title: Species differences in the metabolism of a drug candidate

[1] **Corresponding author:**

M. Reza Anari

Drug Metabolism

Merck Research Laboratories

Sumneytown Pike

P.O. Box 4

PA 19486

TEL: 215 652 0020

E-mail: reza_anari@yahoo.com

# text pages:	19
# tables:	3
# figures:	7
# references:	28
# words in abstract:	1787
# words in introduction:	361
# words in discussion:	1028

Abstract

The pharmacokinetics and metabolism of MRL-A, a selective agonist for the $S1P_1$ receptor, were investigated in rats and dogs. In both species, more than 50% of the dose was excreted in bile. Specific to the rat, and observed in bile, were a taurine conjugate of MRL-A and a glucuronide conjugate of an azetidine lactam metabolite. In dog, a smaller portion of the dose (54% of administered dose) was excreted intact in bile and the major metabolites detected were an azetidine N-oxide of MRL-A and an acylglucuronide of an N-dealkylation product. This latter metabolite was also observed in rat bile. Stereoselective formation of the N-oxide isomer was observed in dogs while the rat produced comparable amounts of both isomers. The formation of a unique glutathione adduct was observed in rat bile, which was proposed to occur via N-dealkylation, followed by reduction of the putative aldehyde product to form the alcohol, and dehydration of the alcohol to generate a reactive quinone methide intermediate. Incubation of a synthetic standard of this alcohol in rat microsomes fortified with reduced glutathione or rat hepatocytes resulted in formation of this unique glutathione adduct.

Introduction

Sphingosine-1-phosphate (S1P) is a lysophospholipid with cell signaling properties that mediates its action through a family of G-protein coupled receptors to elicit its effects on cell function (Fukushima 2001). These S1P receptors are expressed in endothelial, lymphoid, pulmonary, cardiovascular, nervous, and renal tissues. Activation of S1P receptors is implicated in angiogenesis, cardiovascular development, and immune system function (Spiegel & Milstien 2003, Osborne & Stainier 2003). Analogues of S1P, such as FTY 720, have been shown to be agonists of S1P receptors and cause immunosuppression by promoting the sequestration of circulating lymphocytes into secondary lymphoid organs, which results in peripheral lymphopenia and prevents T lymphocyte infiltration of transplanted or antigen-bearing non-lymphoid tissues (Mandala *et al.* 2002, Xie *et al.* 2003). MRL-A is a selective agonist for the $S1P_1$ receptor that is expressed on endothelial and lymphoid tissues. Potential clinical targets for an $S1P_1$ agonist are psoriasis, rheumatoid arthritis, renal transplantation, and multiple sclerosis.

Prior to clinical testing, a new class of therapeutic agent has to be characterized in terms of preclinical metabolism and excretion studies. These disposition investigations are conducted along with safety studies in two animal species (Lin & Lu 1997). Rat as a rodent and dog or monkey as a non-rodent species are commonly utilized for preclinical toxicology and drug metabolism studies. Although all mammals are similar from an evolutionary standpoint because of their common origin, differences in metabolism of drugs are noted amongst various species (Lin *et al.* 1996). This is mainly due to the distinct amino acid sequences of various mammalian isozymes. Even small changes in amino acid sequences are known to give rise to profound differences in substrate specificity (Lindberg and Negishi, 1989). Also differential responses of these isoforms to various environmental and hormonal factors affect the level of expression, rate of metabolism, and the metabolite patterns amongst species.

The purpose of current studies was to characterize the pharmacokinetics and metabolism MRL-A in rats and dogs, the species used during its safety evaluation. Significant quantitative and qualitative differences in metabolism and pharmacokinetics of MRL-A were observed in these two species. A mechanism for formation of a unique glutathione adduct, which was only observed in rats, is proposed.

Materials and Methods

Materials. MRL-A (1-(4-((4-phenyl-5-trifluoromethyl-2-thienyl)methoxy)benzyl)azetidine-3-carboxylic acid, Figure 1, hydrochloride salt), the internal standard for the LC-MS/MS quantitation assay, and synthetic standards of the N-oxide metabolites (mixture of both isomers) and MRL-B, the alcohol synthetic precursor of M10 (Figure 7) were supplied by Medicinal Chemistry at Merck Research Laboratories, Rahway, NJ. The acid standard (M10) was prepared by oxidation of MRL-B with Jones reagent (Shen *et al.*, 2003). [Benzylmethylene-^{14}C]MRL-A (trifluoroacetate salt or hydrochloride salt) was prepared by the Labeled Compound Synthesis Group, Merck Research Laboratories, with the ^{14}C label at the position shown in Figure 1 and a radiochemical purity of >99%. All other chemicals and reagents were of the highest quality available from commercial sources.

In vivo studies. All animal procedures were reviewed and approved by the Merck Research Laboratories Institutional Animal Care and Use Committee. Except where noted, oral (P.O.) doses were administered as suspensions in ethanol: 0.5 % aqueous methylcellulose (20:80, by volume), and intravenous (IV) doses were administered as solutions in ethanol:PEG400:saline (20:40:40, by volume). Blood samples were collected into EDTA-containing tubes and were spun in a centrifuge to obtain plasma. Adult male Sprague Dawley rats (340 – 470 g) and adult male Beagle dogs (10 – 16 kg) were fasted overnight prior to administration of MRL-A. Animals were fed 4 hr postdose, but water was provided *ad libitum*.

Studies in rats. For pharmacokinetic studies, rats were dosed with MRL-A at 1 mg/kg (free acid equivalents) P.O. and 0.5 mg/kg IV (n=4 animals per dose). The rat bile duct cannulated study was conducted in house and the in-life phase of study was conducted at Charles River. For disposition studies, rats were administered a P.O. dose of [^{14}C]MRL-A by gavage at 5 mg/kg (free acid equivalents). The dose was administered with a specific activity of ~32 μCi/mg. In order to obtain larger samples, blood was collected by cardiac puncture for metabolite profiling. Plasma was acidified prior to storage (-70°C)

DMD Fast Forward. Published on May 12, 2006 as DOI: 10.1124/dmd.105.009027
This article has not been copyedited and formatted. The final version may differ from this version.

with 2% v/v formic acid, pH 3 (0.3 mL acid for each mL of plasma) to stabilize potential acyl glucuronide metabolites. Bile duct-cannulated male Sprague-Dawley rats were dosed with [^{14}C]MRL-A at 5 mg/kg P.O. free acid equivalents with a specific activity of ~32 μCi/mg. Bile and urine were collected into pre-tared bottles containing a known volume (indicated in parentheses) of 0.5 M formic acid, pH 3.0 at specified time intervals as follows: pre-dose (0 mL), 0 to 2 (2 mL), 2 to 4 (2 mL), 4 to 8 (4 mL), 8 to 24 (5 mL), 24 to 48 (5 mL), and 48 to 72 (5 mL) hr postdose for bile; and pre-dose, 0 to 8, 8 to 24, 24 to 48, and 48 to 72 hr (5 mL for all samples except predose which contained no acid) postdose for urine. Feces were collected over the same time intervals as urine.

Studies in dogs. For pharmacokinetic studies, dogs were dosed with MRL-A at 1 mg/kg (free acid equivalents) P.O. and 0.5 mg/kg IV (n=4 animals per dose). The bile duct cannulated dog study was performed at Covance. Bile duct-cannulated dogs were dosed with [^{14}C]MRL-A at 1 mg/kg P.O. free acid equivalents (n = 3) with a specific activity of ~20 μCi/mg. Bile was collected into an appropriately sized reservoir that was surrounded by cold packs and connected to the collection catheter via a tether system. Reservoirs contained a known volume of 2% v/v formic acid at specified time intervals as follows: 5 mL per reservoir for the 0 to 2, 2 to 4, 4 to 6, 6 to 8 hr samples, and 15 mL per collection reservoir for the 8 to 24, 24 to 48, 48 to 72, 72 to 96, 96 to 120, 120 to 144 and 144 to 168 hr samples. Urine and feces were collected over the following time periods: 0 to 8, 8 to 24, and then over 24-hr intervals through 168 hr postdose.

In Vitro studies. Rat cryopreserved hepatocytes were obtained from In Vitro Technologies (Baltimore, MD) and defrosted according to their recommended procedures and suspended in 0.1M potassium phosphate, 1mM EDTA buffer, pH 7.4 to a final concentration of 1×10^6 cells/mL. MRL-B was incubated at a concentration of 50 1M with hepatocytes at 37˚C for 60 min in the presence of 5mM glutathione. Reactions were halted with the addition of three volumes of acetonitrile.

Pharmacokinetic studies. Concentrations of MRL-A in rat and dog plasma were determined by LC-MS/MS following protein precipitation with acetonitrile. Calibration curves and quality control (QC) samples were prepared (in triplicate) by mixing 50 µL of control rat plasma with 50 µL of standard solutions prepared in 50% aqueous methanol. Calibration standards, QCs, and postdose plasma (50 µL) were treated with 50 µL of 400 ng/mL internal standard solution in methanol/water (20:80, by volume). This step was followed by protein precipitation with 300 µL of acetonitrile, containing 1% formic acid. Samples were vortex-mixed and spun in a centrifuge for 15 min at 2,000 rpm (at 10°C). The resulting supernatants were analyzed directly by LC-MS/MS. The LC-MS/MS system was comprised of a CTC-PAL Leap Technologies autosampler (Carrboro, NC), two PE200 Binary micro pumps (Perkin Elmer, Norwalk, CT), and a Sciex API 3000 mass spectrometer (PE Sciex, Foster City, CA). Chromatographic separation of the analytes was achieved on a Synergi Max-RP column (2 x 30 mm, 4 µm particle size, Phenomenex, Torrance, CA) with a linear gradient from 95% mobile phase A (aqueous 0.1% formic acid) to 95% mobile phase B (0.1% formic acid in acetonitrile) in 1.5 min and holding at 95% B for 30 sec. Total run time for a single injection was 3.0 min. Mass spectrometric detection of the analytes was accomplished using the Turbo Ionspray interface operated in the positive ionization mode.

Analyte response was measured by multiple reaction monitoring (MRM) of transitions unique to each compound, m/z 448 → m/z 241 for MRL-A and m/z 488 → m/z 387 for the internal standard. Calibration was achieved by plotting the peak area ratios of analyte to internal standard as a function of the nominal concentrations of the standard samples. A line of best fit was generated from the curve points by linear regression with a weighting factor of 1/x2. The lower limit of quantitation (LLOQ) for this assay was 0.95 ng/mL. Pharmacokinetic parameters were calculated using standard noncompartmental methods. Plasma AUC values were calculated using the log-linear trapezoidal method. Extrapolation to infinity was done using the terminal rate constant calculated from the final phase of elimination of the plasma concentration curves for each animal.

DMD Fast Forward. Published on May 12, 2006 as DOI: 10.1124/dmd.105.009027
This article has not been copyedited and formatted. The final version may differ from this version.

Metabolism studies. Concentrations of radioactivity in urine and bile were determined by counting 50-500 µL aliquots mixed with ScintiSafe Gel scintillation cocktail (Fisher Scientific, Pittsburgh, PA) in a Packard Liquid Scintillation Analyzer (Model 1900TR, Downers Grove, IL). Fecal homogenates were prepared following the addition of three to four volumes of water to each collected sample. Aliquots of homogenate (0.2 – 0.5 g) were weighed, allowed to dry overnight, and combusted in a Packard Sample Oxidizer (Model 307, Perkin Elmer Bioscience). Oxidized carbon-14 was trapped as [^{14}C]-carbamate that was measured subsequently by liquid scintillation counting.

Proportionate 0-72 hr pools of urine, fecal homogenate and bile were prepared from each rat and dog according to the volume or weight excreted at each time interval. For the analysis of bile and fecal homogenates, 0.5-2 mL aliquots were mixed with 3 volumes of acetonitrile. After centrifugation, the supernatant was evaporated to dryness under a stream of N_2 and reconstituted in 0.2-0.5 mL methanol:water (75:25, by volume). For metabolite profiling of urine, 2 mL aliquots of pooled sample from each animal were evaporated to dryness under a stream of N_2, reconstituted in 0.2-0.4 mL 50% aqueous methanol and analyzed by LC-MS/MS (*vide infra*). An equal volume of acidified plasma from each animal was pooled at each timepoint and precipitated with ~2 - 8 volumes of acetonitrile. Following centrifugation (~2000 × g, 10 min, 4°C), the supernatant was evaporated to dryness under a stream of N_2 and reconstituted in 200 – 500 µL methanol:water (75:25, by volume). Equal volumes of reconstituted samples from each animal were mixed prior to LC-MS analysis to generate a single sample of bile, urine, or feces for each dosing route.

The LC-MS/MS system for metabolite profiling consisted of a Shimadzu SIL-10ADvp autosampler, a Shimadzu SCL-10Avp system controller, two Shimadzu LC-10ADvp pumps (Columbia, MD), a ThermoFinnigan LCQ Classic ion trap mass spectrometer (San Jose, CA), and either a Beta-Ram

radioactivity flow detector (IN/US Systems Inc., Tampa, FL) or a Packard 500TR flow scintillation analyzer (Perkin Elmer Life and Analytical Sciences, Shelton, CT). The mobile phases were A, 0.1% formic acid in water, and B, acetonitrile plus 0.1% formic acid.

For *in vivo* samples, a Synergi Max-RP column (2 x 150 mm; 4 μm from Phenomenex, Torrance, CA) was used for chromatographic separation. The gradient was begun at 30% B and held at 30% B for 2 min, increased linearly to 45% B over the next 38 min, and held at 45% B for 5 min, increased to 90%B over 5 min, followed by a hold at 90% B for 5 min. The effluent from the column, eluted at a rate of 0.3 mL/min, was diverted, at a 5:1 ratio, into the radioactive flow detector and the mass spectrometer, respectively. Scintillation cocktail (Packard Ultima Flo-M) was pumped at a rate of 1 mL/min into the radiometric detector. For samples containing low concentrations of radioactivity, the eluant was collected at 1-min intervals and mixed with Scintisafe Gel scintillation cocktail prior to liquid scintillation counting.

For *in vitro* samples, a Discovery HSC18 column (4.6 x 150 mm; 3 μm from Supelco, Bellfonte, PA) was used for chromatographic separation. The gradient was begun at 25% B and held for 10 min, increased linearly to 70% B over the next 40 min, and increased to 90%B over 5 min, followed by a hold at 90% B for 5 min. The effluent from the column, eluted at a rate of 1 mL/min, was diverted, at a 5:1 ratio, into the radioactive flow detector and the mass spectrometer, respectively. Scintillation cocktail (Packard Ultima Flo-M) was pumped at a rate of 3 mL/min into the radiometric detector.

Metabolites of [^{14}C]MRL-A were identified using the ion trap mass spectrometer in the positive electrospray mode, except for M8 and M10 which could only be detected by negative electrospray. The ionization mode, retention times, and fragmentation pattern for MRL-A were established using an ethanolic solution of synthetic standard. The CID spectra of the metabolites were obtained in a data-

dependent and list-dependent mode. Product ion scans of selected metabolites were obtained as needed for further confirmation of their identity.

Incubation of dog bile with rat intestinal contents. The section of intestine that extends 5 cm on either side of the caecum was excised from anesthetized rats that had been fasted and cut open lengthwise to expose the contents. The tissue was placed in three volumes of buffer (50 mM Tris, 1.15% KCl, pH 7.4) and stirred to release contents. A 200 μL aliquot of pooled dog bile was incubated with 10 volumes of the intestinal content suspension at 37ºC for 18 hours under a nitrogen atmosphere, after which time it was quenched with six volumes of acetonitrile. Following centrifugation, the supernatant was evaporated to dryness under a stream of N_2 and reconstituted in 0.2 mL methanol:water (75:25, by volume) and analyzed by LC-MS/MS as described for metabolite studies (*vide supra*).

Isolation of M8. Metabolite M8 was isolated from 50 mL of bile from intravenously and orally dosed dogs. Bile was subjected to treatment with 3 volumes of acetonitrile and spun in a centrifuge. After evaporation of the supernatant, the residue was reconstituted in 50 mL water and subjected to solid phase extraction on a 10-g Bond Elut C18 cartridge (Varian, Walnut Creek, CA). The sample was loaded onto the cartridge, which had been washed with 25 mL water, and the analyte of interest was eluted with 25 mL acetonitrile. The eluant was evaporated to dryness under a stream of N_2 and reconstituted in methanol:water (75:25, by volume). Metabolite M8 was isolated from the extract by HPLC analysis on a semi-preparative scale column. A Synergi Max-RP column (10 x 250 mm; 4 μm from Phenomenex) was used for chromatographic separation. The same gradient was used as for metabolite profiling (*vide supra*). The effluent from the column, eluted at a rate of 4.0 mL min^{-1}, was collected at 1-min intervals. An aliquot (50 μL) of each fraction was assayed for its radioactive content after mixing with 6 mL of ScintiSafe Gel scintillation cocktail. The fractions of interest, based on retention time and radioactivity,

were pooled and evaporated to dryness under a stream of N_2. The residue was reconstituted in 200 µL methanol:water (75:25, by volume).

The isolated metabolite was further purified in two steps using analytical-scale HPLC, using the same gradient and mobile phases as were used for the isolation step (*vide supra*). The columns (both from Phenomenex) used were Synergi Max-RP column (2 x 150 mm) and Synergi Polar-RP column (2 x 150 mm) and the elution rate was 0.3 mL min^{-1} for both columns. After each chromatography run, aliquots of the fractions were counted, and the radioactive fractions were pooled and dried under N_2. The residues were reconstituted in 200 µL methanol:water (75:25, by volume) in preparation for injection onto the next column.

Proton NMR spectra of metabolite M8, as well as the parent compound, were obtained in acetonitrile-d_3 and acetonitrile-d_3:D_2O (8:1, by volume) at room temperature using a Varian Inova 600 MHz NMR spectrometer in a 3 mm Nalorac probe. A portion of the metabolite was infused directly into the ion trap mass spectrophotometer to obtain full scan and product ion scan spectra under negative ionspray conditions. Approximately 500 ng of the isolated metabolite was incubated with 200 units β-glucuronidase (from E. coli, supplied by Sigma, St. Louis, MO) overnight at 37°C in 8 mM potassium phosphate buffer, pH 6.8. The reaction was halted by the addition of two volumes of acetonitrile. After centrifugation, the supernatant was evaporated to dryness under a stream of N_2 and the residue was reconstituted in 0.2 mL methanol:water (75:25, by volume). The retention time and MS fragmentation pattern of the hydrolysis product under negative ionspray conditions were compared with the corresponding parameters of a synthetic standard of M10.

Results

Pharmacokinetic studies

Following intravenous administration (0.5 mg/kg) of MRL-A, plasma clearance was 20 mL/ min/kg in rats and 3.1 mL/min/kg in dogs (Table 1). The terminal half-life ($T_{1/2}$) was 10 hr in dogs and 6.8 hr in rats and the volume of distribution in was 10.6 L/kg in rats compared to 2.0 L/kg in dogs. Following oral administration (1 mg/kg), the area under curve (AUC) of plasma concentration vs. time profile and maximum plasma concentration (C_{max}) values were much lower in rat (1.5 μM.hr and 0.1 μM) compared to the values in dogs (10.7 μM.hr and 1.5 μM), consistent with the higher plasma clearance in the rats. MRL-A was well absorbed and its estimated bioavailability ranged from 83 to 86% in both species. After oral dosing, absorption of MRL-A was more rapid in dogs than in rats, with time to maximum plasma concentrations (T_{max}) achieved 2 hr postdose. Therefore, the pharmacokinetic studies revealed that significant inter-species differences exists in the rate of plasma clearance of MRL-A between rat and dog, which translated in to major differences in AUC (7-fold) and C_{max} (10-fold).

Excretion studies

Following oral administration of [^{14}C]MRL-A to bile duct-cannulated male Sprague-Dawley rats (5 mg/kg), approximately 88% of the radioactive dose was recovered in 72 hr (Table 2). The excretion pattern indicated that 72% of the dose was eliminated via the bile and approximately 1.4% of the dose was eliminated via the kidneys in to the urine. Thus, ~74% of the dose was absorbed in this study. Following oral administration of [^{14}C]MRL-A (1 mg/kg) to bile duct-cannulated male beagle dogs, approximately 80% of the dose was recovered in 168-hr. As with rats, the primary route of elimination was via biliary elimination (54%) (Table 2), with the largest portion of the radioactivity excreted in the first 48 hours postdose. Less than 4% of an oral dose was excreted into the urine. About 20% of the dose was recovered in the feces, which indicated a good oral absorption in dogs (~58%).

DMD Fast Forward. Published on May 12, 2006 as DOI: 10.1124/dmd.105.009027
This article has not been copyedited and formatted. The final version may differ from this version.

Metabolite Profiles

Bile, urine and feces from rats dosed with [^{14}C]MRL-A at 5 mg/kg P.O. were analyzed for metabolites. Parent compound was the major radioactive component in bile, where it represented 26% of the total radioactivity excreted in 72 hr (Figure 2A). The taurine conjugate of parent compound (M5, ~20% of radioactivity in bile) was the most abundant metabolite followed by the azetidine lactam glucuronide (M9, 14% of radioactivity in bile). Other minor metabolites identified by LC-MS/MS were labeled M1 through to M11 and listed in Table 3. The remaining minor metabolites each accounted for less than 10% of the radioactivity excreted in bile. Of particular note, the formation of a glutathione adduct, M7 was detected in rat bile as 2 – 3 % of the administered dose. The mechanism for the formation of this metabolite was investigated further *in vitro (vide infra)*. Feces collected from the same rats contained only parent MRL-A and the radioactivity excreted into rat urine (~1% of dose) eluted in the void volume of the column and was not investigated further. Rat plasma contained primarily unchanged parent (>63% of circulating radioactivity up to 48 hr post-dose) and also the taurine (M5) and lactam (M11) metabolite.

In dogs dosed with [^{14}C]MRL-A at 1 mg/kg P.O., one of the azetidine *N*-oxide isomers (M6) was the major radioactive component in bile, and it represented 52% of the total radioactivity excreted in 168 hr (Figure 2B). The acyl glucuronide of the N-dealkylation acid product (M8) (26%) was the next most abundant radioactive component in bile followed by the unchanged parent compound (13%). Other minor metabolites (<10% of excreted radioactivity) included the azetidine *N*-oxide isomer (M4) and the sulfate conjugate of a hydroxylated metabolite (M1), which was previously detected in rat bile. Metabolites that were not observed in the dog included M2 (which presumably is actually formed as a by-product of N-dealkylation since M10 is observed in dog bile and plasma), M3 (the acylglucuronide of MRL-A), M7, M9, and M11 (Table 3). Low levels of parent MRL-A and the azetidine *N*-oxide isomers, M4 and M6, were detected in dog urine (<10% of urine radioactivity) while the dog feces only contained MRL-A and M10. Incubation of dog bile with rat intestinal contents altered the metabolite profile so that it mimicked the metabolite profile observed in dog feces. Most likely, the intestinal contents reduced the

N-oxide back to parent MRL-A and hydrolyzed the acylglucuronide M8 to M10. The hydrolysis experiment with intestinal contents provided indirect evidence that dog feces contain the N-dealkylation acid product (M10) in addition to parent compound. Parent compound was the major drug-related component in plasma, representing >80% of circulating radioactivity up to 8 hr after P.O. administration. The isomeric azetidine *N*-oxide metabolites (M4 and M6) were detected as minor metabolites in dog plasma.

Identification of Metabolites

The CID spectrum of MRL-A and its major fragment ions are shown in Figure 3. The two major fragment ions at *m/z* 347 and *m/z* 241 correspond to the loss of the azetidine carboxylic acid moiety and subsequent loss of the adjacent phenolmethylene moiety, respectively. Further fragmentation of the 2-trifluoromethyl-3-benzyl thiophene group, *m/z* 241, resulted in the loss of -HF (20Da) to *m/z* 221 or neutral loss of 69 Da, the entire trifluoromethyl group, to yield *m/z* 172. Profiles of biological samples were obtained by HPLC with flow scintillation analysis for radioactivity. Radioactive peaks were analyzed by on-line mass spectrometry to identify metabolite structures as summarized in Table 3. A metabolism scheme showing the structures of these metabolites is displayed in Figure 6.

Identification of M1. Metabolite M1 gave a protonated molecular $[M+H]^+$ ion at *m/z* 544. Fragmentation of this ion gave rise to *m/z* 443 and *m/z* 337, which indicated the addition of 96 Da to the 2-trifluoromethyl-3-benzyl thiophene group. The loss of 80 Da, corresponding to a sulfate group, was observed upon fragmentation of molecular ion *m/z 544* as *m/z* 464 or upon further fragmentation of ion *m/z* 337 to *m/z* 257. The fragment ion *m/z* 188 (i.e. 172 + 16) further confirms the addition of a hydroxyl group to the 2-trifluoromethyl-3-benzyl thiophene group. These data led to the assignment of M1 as a sulfate conjugate of a hydroxylated metabolite.

DMD Fast Forward. Published on May 12, 2006 as DOI: 10.1124/dmd.105.009027
This article has not been copyedited and formatted. The final version may differ from this version.

Identification of M2. The product ion spectrum of M2 (*m/z* 364) was identical to that of parent compound, indicating that the loss of 84 Da was from the azetidine carboxylic acid portion of the molecule. The loss of 17 Da to generate fragment *m/z* 347 could suggest either a primary amine or alcohol functional group attached to the benzylmethylene carbon. The retention time of the metabolite was compared to a synthetic standard of the alcohol but it did not match. Therefore, M2 was proposed to be the primary amine.

Identification of M3. M3 had a protonated molecular $[M+H]^+$ ion at *m/z* 624 consistent with a glucuronide conjugate of parent compound. The product ion spectrum of M3 afforded the two characteristic fragments of parent compound *m/z* 347 and *m/z* 241. The carboxylic acid group is the most likely position for glucuronidation on this molecule and the relative retention time of the glucuronide metabolite to the aglycone parent compound is consistent with acylglucuronidation (cf. M8 with respect to M10).

Identification of M4 and M6. Two radioactive peaks, M4 and M6, both had a protonated molecular $[M+H]^+$ ion at *m/z* 464. The fragmentation pattern of these ions was identical to parent compound. Comparison to authentic standards mix confirmed that both were azetidine N-oxide metabolites. Two conformations of the N-oxide are possible because the oxygen can be positioned *cis*- or *trans*- with respect to the carboxylic acid attached to the azetidine ring. Both M4 and M6 could be separated by LC, with M4 being detected in both rat and dog bile, but M6 was observed only in dog bile.

Identification of M5. Metabolite 5 gave a protonated molecular $[M+H]^+$ ion at *m/z* 555, which is 107 Da greater than the parent compound. The product ion spectrum of M5 contained the diagnostic fragments of parent compound *m/z* 347 and *m/z* 241. However, the fragment ion corresponding to parent compound was absent. Instead, *m/z* 449 was detected which is 1 Da greater than parent compound. This is possible if the –OH of the carboxylic functional group was replaced with $–NH_3^+$. Based on this information, a

taurine conjugate was proposed containing an amide bond linkage between the taurine group and the azetidine ring.

Identification of M7. M7 resulted from modification near the azetidine ring because the product ion spectrum of M7 (*m/z* 654) contained the two characteristic fragments of parent compound *m/z* 347 and *m/z* 241 but not *m/z* 448. Neutral losses of 75 Da and 129 Da gave rise to *m/z* 579 and *m/z* 525, respectively, suggesting the presence of a glutathione adduct. Complete loss of the glutathione would correspond to *m/z* 347; consequently, M7 was assigned as a benzylmethylene glutathione adduct which had lost the azetidine carboxylic acid group. We propose that the formation of the glutathione adduct arises from N-dealkylation followed by dehydration to generate a reactive quinone methide intermediate (Figure 7). To test this hypothesis, the alcohol analogue MRL-B was incubated with rat hepatocytes in the presence of excess glutathione to trap the reactive intermediates and detect the glutathione adducts formed. The formation of M7 was detected from incubations of MRL-B with rat hepatocytes and liver microsomes (data not shown).

Identification of M8. Metabolite 8 could not be identified under positive ionspray conditions. This metabolite was isolated and purified from dog bile for analysis using ^{1}H NMR (Figure 4). The proposed metabolite structure was based on the absence of the signal of the methylene protons at position **e** and a downfield shift of the aromatic protons at position **d** suggesting the presence of an electron withdrawing group, such as a carbonyl group, at position **e**. The signal for the protons of the azetidine ring at position **f** also was absent, indicating the loss of this portion of the molecule. The presence of the anomeric proton of the glucuronic acid moiety is indicative of a β-1-O-acyl conjugate. Based on this information, a deprotonated molecular ion $[M-H]^-$ at *m/z* 553 was detected by negative ion mode MS of the isolated metabolite. The product ion scan of this ion contained fragment *m/z* 377, corresponding to the loss of the glucuronide conjugate (Figure 5). Neutral loss of the carboxylic acid functional group to form m/z 333 was observed upon further fragmentation of *m/z* 377. As a result, M8 was proposed to be an

acylglucuronide conjugate of an N-dealkylation acid product that arose from the loss of the azetidine carboxylic acid group.

Identification of M9. Metabolite M9 (*m/z* 638) was observed to undergo neutral loss of 176 Da and subsequent loss of HF to form m*/z* 462 and *m/z* 442, respectively, during collision-induced dissociation. Oxidation of the azetidine ring to a lactam was proposed because the second-generation fragment *m/z* 316 (from *m/z* 442) was assigned as the loss of 1-methylazetidine-3-carboxylic acid containing an additional 14 Da. The second-generation fragment *m/z* 296 was proposed to be formed by an additional loss of HF. These data are consistent with formation of an azetidine lactam acylglucuronide metabolite (see identification of M11 below).

Identification of M10. Hydrolysis of the glucuronide conjugate, M8, led to the identification of the N-dealkylation acid product, M10. Formation of M10 from M8 was observed when dog bile was incubated with rat intestinal contents and the same metabolite was formed when purified M8 was incubated with β-glucuronidase (data not shown). A mass spectrum of M10 could be observed for the hydrolyzed product only under negative electrospray conditions. The deprotonated molecule $[M-H]^-$ was observed at *m/z* 378 and, as with M8, the product ion spectrum contained the fragment *m/z* 333 corresponding to the loss of the carboxylic acid group. The 2-trifluoromethyl-3-benzyl-thiophene moiety was detected as the second generation fragment *m/z* 227 upon further fragmentation of *m/z* 333. The retention time and mass spectra were identical to those of a synthetic standard.

Identification of M11. M11 was detected in rat bile when identifying metabolites in positive ion mode and was found to have the same retention time as M10. The protonated molecular ion $[M+H]^+$ was detected at *m/z* 462. Fragmentation of this ion produced a major fragment *m/z* 442 (loss of HF) in addition to the less intense fragment *m/z* 241. The formation of a lactam was proposed for M11 since the

fragmentation pattern was similar to M9 and the addition of 14Da to the azetidine carboxylic acid portion likely would occur as the addition of a carbonyl group at that position.

Discussion

Preclinical drug metabolism studies were conducted on the $S1P_1$ receptor agonist, MRL-A, and included the determination of pharmacokinetic parameters, routes of excretion for drug-related material, and characterization of metabolites in plasma and excreta. Using male rats and dogs as preclinical models, significant differences in the disposition of MRL-A were observed between the two species. The plasma clearance of MRL-A was much faster in rats (20 mL/min/kg) than in dogs (3 mL/min/kg). This resulted in a longer half life and higher plasma concentrations for MRL-A in the dog. The basis for such species differences was further investigated by detailed metabolism and excretion studies in both rats and dogs.

Following IV or P.O. dosing of [^{14}C]MRL-A to rats and dogs, >50% of the dose was eliminated via the bile. For this reason, the biotransformation of MRL-A was investigated primarily by the identification of biliary metabolites. Taurine conjugation of MRL-A to form M5 (Figure 2), or a combination of oxidation and glucuronidation to form the azetidine lactam acyl glucuronide metabolite of MRL-A (M9, Figure 2) each represented major (≥14% of the radioactivity in bile) and species specific metabolic routes for MRL-A in the rat. Conversely stereoselective azetidine *N*-oxidation (to form M6, Figure 2) represented the major (>50% of total radioactivity eliminated in bile) metabolic route for MRL-A in the dog, although the alternative N-oxide isomer (M4) was observed in both species (Table 3). In both rat and dog, MRL-A did undergo azetidine N-dealkylation although in the dog the downstream end product of this reaction, the carboxylic acid (M10), was excreted as the acyl glucuronide M8 (Figure 2).

Carboxylic acid-containing xenobiotics are often eliminated following conjugation with either an amino acid (*e.g.* glycine, taurine or glutamine) or with glucuronic acid. In general, taurine conjugation is perceived to be a high affinity, low capacity system (Mulder 1990), whereas conjugation with glucuronic acid is considered to be a high capacity process with broad substrate specificity (Hutt and Caldwell, 1990). In the case of a β_3-adrenergic receptor agonist, Tang *et al.* (2002) postulated that preferential conjugation by taurine or isethionic acid was observed as a result of the limited availability of the

precursor carboxylic acid metabolite. In their study, direct *in vivo* administration of the carboxylic acid metabolite to rats at higher concentrations led to a combination of amino acid and glucuronic acid conjugation. In addition, saturation of taurine conjugation with a corresponding increase in glucuronic acid conjugation of a PPAR agonist was observed with increasing dose in dogs (Kim *et al*. 2004). A switch from amino acid (glycine) conjugation to glucuronic acid conjugation was also observed with increased doses following administration of 1-naphthylacetic acid to rats (Dixon et al. 1977). Furthermore, salicylate conjugation by glycine to salicyluric acid is saturated at therapeutic doses in man (Levy 1965a, b). However, in the case of MRL-A, we did not observe any evidence that the amino acid conjugation pathway was being saturated when the dose was increased from 1 to 45 mg/kg P.O. (data not shown). We propose that MRL-A is either not a substrate for dog acyl coenzyme A, the key activating step in amino acid conjugation with, in this instance taurine, or has preferential affinity for N-oxidation likely to be mediated by the FMO family of enzymes.

Oxidation of the azetidine ring to form lactam metabolites was more predominant in the rat while in the dog, MRL-A was more susceptible to N-oxidation or oxidation of the adjacent methylene group leading to *N*-dealkylation. Furthermore, stereoselective formation and elimination of M6 was detected in dog bile, while rat bile and plasma contained comparable amounts of both isomers. In addition to CYP enzymes, *N*-oxidations often are found to be catalyzed by FMO enzymes. Cases of stereoselective *N*-oxidation of tertiary amines by FMO enzymes have been reported for N-ethyl-N-methylaniline (Hadley *et al.* 1994a), pargyline (Hadley *et al.* 1994b), as well as (S)-nicotine (Damani *et al.* 1988, Cashman *et al.* 1992) and its bioisostere, ABT-418 (Rodrigues *et al.* 1995). Expression of different FMO enzymes is the likely reason that there are species differences in the stereoselectivity in the N-oxidation of (S)-nicotine (Cashman 2000) but one cannot exclude the possibility of stereoselective reduction of *N*-oxides back to parent (Rodrigues *et al.* 1995).

The glutathione adduct, M7, represented a metabolite that was unique to rats. GSH adduct formation is indicative of a reactive intermediate of MRL-A having been formed (Evans *et al*. 2004). We have demonstrated that M7 can be formed *in vitro* following incubation of MRL-B with glutathione in rat hepatocytes. One possible mechanism is that MRL-B undergoes P450-catalyzed dehydration to form the *p*-quinone methide intermediate that is subsequently trapped by glutathione. Mammalian microsomal enzymes are known to catalyze these reactions with model aldoximes, e.g., P450 3A4 (Boucher *et al*. 1994). Quinone methides are known reactive intermediates that form covalent adducts with protein and DNA and have been implicated in the pulmonary toxicity of butylated hydroxytoluene, the hepatocarcinogenicity of safrole, and the hepatotoxicity of eugenol (Monks and Jones, 2002). There are several possible ways by which one would envision the formation of the GSH conjugate. We propose that MRL-B could be formed by reduction of the putative aldehyde that is formed following azetidine N-dealkylation of MRL-A, a pathway we know to exist in the rat by virtue of M8 being detected in rat bile. M8 was a relatively minor metabolite (<10% radioactivity in bile) and following a safety assessment study in rats (5, 15, 45 mg/kg/day of MRL-A for 16 days) no liver toxicity was observed.

These studies also serve to confirm the need for biliary excretion studies in the investigation of biotransformation and elimination of xenobiotics. The ability of the gut contents to reconvert *N*-oxides to their precursor and deconjugated metabolites has been well documented (Jaworski *et al.* 1991, Dickinson and King 2001, Roberts *et al*. 2002). Metabolite profiles from feces alone may mislead investigators from identifying the biotransformation pathway responsible for the elimination of the compound into bile and, in this case, mask the species differences in metabolism. For MRL-A, the fecal metabolite profiles from rats and dogs were identical even though there were dramatic differences in the metabolites that were excreted into the bile from these two species.

Acknowledgements

The authors would like to thank Drs. Jeff Hale and Ross Miller who provided MRL-A and MRL-B for evaluation, and to Anson Chang, Herbert Jenkins, and Yolanda Jakubowski for their analysis of the ^{14}C-labeled material. In addition, we are grateful for the assistance of Lauren Marshall in the isolation of M8 from dog bile. We would like to acknowledge that the in-life phase of the biliary study in dogs was conducted at Charles River Laboratories. Appreciation is also extended to Ron Franklin for his critical review of this manuscript.

References

Boucher JL, Delaforge M, and Mansuy D (1994) Dehydration of alkyl- and arylaldoximes as a new cytochrome P450-catalyzed reaction: mechanism and stereochemical characteristics. *Biochemistry* **33**, 7811-7818.

Cashman JR, Park SB, Yang Z-C, Wrighton SA, Jacob P, and Benowitz NL (1992) Metabolism of nicotine by human liver microsomes: stereoselective formation of trans-nicotine N'-oxide. *Chem Res Toxicol*. **5**: 639-646.

Cashman JR (2000) Human Flavin-Containing Monooxygenase: Substrate Specificity and Role in Drug Metabolism. *Current Drug Metabolism* **1**(2): 181-191.

Damani LA, Pool WF, Crooks PA, Kaderlid RK, and Ziegler DM (1988) Stereoselectivity in the N-oxidation of nicotine isomers by flavin-containing monooxygenase. *Mol. Pharmacol*. **33**: 702-705.

Dickinson RG and King AR (2001) Rearrangement of diflunisal acyl glucuronide into its β-glucuronidase-resistant isomers facilitates transport through the small intestine to the colon of the rat. *Life Sciences* **70**: 25-36.

Dixon PAF, Caldwell J, and Smith RL (1977) Metabolism of arylacetic acids. 1. The fate of 1-naphthylacetic acid and its variation with species and dose. *Xenobiotica* **7**: 695-706.

Evans DC, Watt AP, Nicoll-Griffith DA, and Baillie TA (2004) Drug-Protein Adducts: An industry perspective on minimizing the potential for drug bioactivation in drug discovery and development. *Chem. Res. Toxicol*. **17**: 3-16.

Fukushima N, Ishii I, Contos JJA, Weiner JA, and Chun, J (2001) Lysophospholipid Receptors. *Annu. Rev. Pharmacol. Toxicol*. **41**: 507-34.

Hadley MR, Oldham HG, Damani LA, and Hutt AJ (1994a) Asymetric metabolic N-oxidation of N-ethyl-N-methylaniline by purified flavin-containing monooxygenase. *Chirality* **6**(2): 98-104.

Hadley MR, Svajdlenka E, Damani LA, Oldham HG, Tribe J, Camilleri P, and Hutt AJ (1994b) Species variability in the stereoselective N-oxidation of pargyline. *Chirality* **6**(2): 91-97.

Hutt AJ and Caldwell J (1990) Amino acid conjugation. In, GJ Mulder (ed.), Conjugation Reactions in Drug Metabolism, pp.273-305, Taylor & Francis, London.

Jaworski TJ, Hawes EM, Hubbard JW, Mckay G, and Midha KK (1991) The metabolites of chlorpromazine N-oxide in rat bile. *Xenobiotica* **21**(11): 1451-1459.

Kim M- S, Shen Z, Kochansky C, Lynn K, Wang S, Wang Z, Hora D, Brunner J, Franklin RB, and Vincent SH (2004) Differences in the metabolism and pharmacokinetics of two structurally similar PPAR agonists in dogs: involvement of taurine conjugation. *Xenobiotica* 34(7): 665-674.

Levy G (1965a) Salicylurate formation demonstration of Michaelis-Menten kinetics in man. *J Pharm Sci* **54**: 496.

Levy G (1965b) Pharmacokinetics of salicylate elimination in man. *J Pharm Sci* **54**: 959-967.

Lin JH, Lu AY (1997) Role of pharmacokinetics and metabolism in drug discovery and development. *Pharmacol Rev* **49**: 403-449.

Lin JH, Chiba M, Balani SK, Chen IW, Kwei GY, Vastag KJ, Nishime JA (1996) Species differences in the pharmacokinetics and metabolism of indinavir, a potent human immunodeficiency virus protease inhibitor. *Drug Metab Dispos* **24**: 1111-1120.

Lindberg and Negishi (1989) Alteration of mouse cytochrome P450coh substrate specificity by mutation of a single amino-acid residue. *Nature* **339**: 632-634.

Mandala S, Hajdu R, Bergstrom J, Quackenbush E, Xie J, Milligan J, Thorton R, Shei G-J, Card D, Keohane CA, Rosenback M, Hale J, Lynch CL, Rupprecht K, Parsons W, and Rosen H (2002) Alteration of Lymphocyte Trafficking by Sphingosine-1-Phosphate Receptor Agonists. *Science* **296**: 346-349, 2002.

Monks TJ and Jones DC (2002) The Metabolism and Toxicity of Quinones, Quinonimines, Quinone Methides, and Quinone-Thioethers. *Current Drug Metabolism*. **3**: 425-438.

Mulder GJ (1990) Competition between conjugations for the same substrate, in *Conjugation Reactions in Drug Metabolism* (Mulder GJ ed.) pp 41-49, Taylor & Francis, London.

Osborne N and Stainier DY (2003) Lipid receptors in cardiovascular development. *Annu. Rev. Physiol.* **65**: 23-43.

Roberts MS, Magnusson BM, Burczynski FJ, and Weiss M (2002) Enterohepatic Circulation: Physiological, Pharmacokinetc and Clinical Implications. *Clin. Pharmacokinet.***41**(10): 751-790.

Rodrigues AD, Kukulka MJ, Ferrero JL, and Cashman JR (1995) In Vitro Hepatic Metabolism of ABT-418 in chimpanzee (Pan Troglodytes): A unique pattern of microsomal flavin-containing monooxygenase-dependent stereoselective N-oxidation. *Drug Metab Dispos* **23**(10): 1143-1152.

Shen Z, Reed JR, Creighton MD, Liu DQ, Tang YS, Hora DF, Feeney W, Szeczyk J, Bakhtiar R, Franklin RB, and Vincent SH (2003) Identification of novel metabolites of pioglitazone in rat and dog. *Xenobiotica*. **33**(5): 499-509.

Spiegel S and Milstien S (2003) Sphingosine-1-phosphate: An enigmatic signalling lipid. *Mol. Cell Biol.* **4**(5): 397-407.

Tang W, Stearns RA, Miller RR, Ngui JS, Mathvink RJ, Weber AE, Kwei GY, Strauss JR, Keohane CA, Doss GA, Chiu SHL, and Baillie TA (2002) Metabolism of a Thiazole Benzenesulfonamide Derivative, A Potent and Selective Agonst of the Human ϑ_3-adrenergic receptor, in Rats: Identification of a Novel Isethionic Acid Conjugate. *Drug Metab and Dispos* **30**(7): 778-787.

Xie JH, Nomura N, Koprak SL, Quackenbush EJ, Forrest MJ, Rosen, H (2003) Sphingosine-1-Phosphate Receptor Agonism Impairs the Efficiency of the Local Immune Response by Altering Trafficking of Naive and Antigen-Activated $CD4^+$ T Cells. *J Immunol.* **170**(7): 3662-3670.

Footnotes

[1] **Sent reprint requests to:**

M. Reza Anari

Department of Drug Metabolism

Merck Research Laboratories

Sumneytown Pike

P.O. Box 4

PA 19486

TEL: 215 652 0020

E-mail: reza_anari@yahoo.com

[2] Current address: Amgen Inc., One Kendall Sq. Bldg, 1000, Cambridge, MA 02139

[3] Current address: Drug Metabolism, Johnson & Johnson PRD, Raritan, NJ 08869

Figure Titles/Captions

Figure 1. Chemical structure of MRL-A, 1-(4-((4-phenyl-5-trifluoromethyl-2-thienyl) **(A)** methoxy)benzyl)azetidine-3-carboxylic acid (A), the internal standard used for plasma quantitation (B), and MRL-B, the alcohol precursor of M10 (C). Asterisk in the structure indicates location of 14-C labeling.

Figure 2. HPLC radiochromatograms of (A) rat bile following administration of [^{14}C]MRL-A at 5 mg/kg P.O., (B) dog bile following administration of [^{14}C]MRL-A at 1 mg/kg P.O.

Figure 3. (A) Mass spectrum of MRL-A (B) Product ion mass spectrum of MRL-A *m/z* 448 and the proposed assignment of fragment ions (C) Product ion mass spectrum of fragment *m/z* 241 and the proposed assignment of fragment ions.

Figure 4. NMR spectra of metabolite M8 isolated from dog bile (A) and parent compound MRL-A (B)

Figure 5. (A) MS2 product ion mass spectrum of metabolite M8 (*m/z* 553) isolated from dog bile (B) MS3 product ion mass spectrum of fragment *m/z* 377 from metabolite M8

Figure 6. In Vivo Metabolism of [14C]MRL-A in rats and dogs

Figure 7. Proposed metabolism of MRL-A to form M10 and the glutathione adduct, M7. *N*-dealkylation of MRL-A is observed in rats and dogs as the formation of M10 (dogs) or M8 (rats). Reduction of the aldehyde intermediate is presumed to represent an alternative pathway. We have demonstrated that M7 can be formed *in vitro* following incubation of MRL-B with

glutathione in rat hepatocytes and propose that this transformation occurs via dehydration to form the *p*-quinone methide intermediate.

DMD Fast Forward. Published on May 12, 2006 as DOI: 10.1124/dmd.105.009027
This article has not been copyedited and formatted. The final version may differ from this version.

Table 1
Pharmacokinetic parameters of MRL-A in rats and dogs [a]

IV Dose (mg/kg)	**$AUC_{0-\infty}$ (μM·hr)**	**Cl_p (mL/min/kg)**	**Vd_{ss} (L/kg)**	**$T_{1/2}$ (hr)**
Rats (n=4)				
0.5	0.9 ± 0.1	20.3 ± 1.0	10.6 ± 0.6	6.8 ± 0.7
Dogs (n=3)				
0.5	6.2 ± 1.4	3.1 ± 0.7	2.0 ± 0.2	10.0 ± 0.2

Oral Dose (mg/kg)	**$AUC_{0-\infty}$ (μM·hr)**	**C_{max} (μM)**	**T_{max} (hr)**	**F (%)**
Rats (n=4)				
1	1.5 ± 0.5	0.1 ± 0.0	5.0 ± 1.2	83
Dogs (n=3)				
1	10.7 ± 3.3	1.0 ± 0.3	2.0 ± 0.0	86 [b]

[a] Rats and dogs were dosed intravenously with a solution of the hydrochloride salt in ethanol:PEG400:saline (20:40:40) or orally with a suspension of the hydrochloride salt in 20% ethanol: 80% methylcellulose (0.5% w/v). Data are listed as the mean ± standard deviation.

[b] Bioavailability of 1 mg/kg dose in dogs was determined individually for each dog in a cross over experiment with the same dogs dosed intravenously at 0.5 mg/kg.

DMD Fast Forward. Published on May 12, 2006 as DOI: 10.1124/dmd.105.009027
This article has not been copyedited and formatted. The final version may differ from this version.

Table 2
Dose Recovery (%) in Bile, Urine, and Feces Following Oral Administration of [^{14}C]MRL-A to rats (5 mg/kg) and dogs (1 mg/kg) [a]

Sample	Dose (%)	
	Rats (0-72 hr, n=3)	**Dogs (0-168 hr, n=3)**
Bile	72 ± 2.8	54 ± 29
Urine	1.4 ± 0.2	3.5 ± 2.4
Feces	15 ± 3.7	20 ± 6.8
Total	88 ± 1.6	80 ± 19

[a] Values represent mean ± standard deviation.

DMD Fast Forward. Published on May 12, 2006 as DOI: 10.1124/dmd.105.009027
This article has not been copyedited and formatted. The final version may differ from this version.

Table 3
Metabolites of [^{14}C]MRL-A detected in various biological matrices *in vitro* and *in vivo*[a]

Metabolite Label	Proposed Metabolites	m/z	MS2[b]	MS3[c]	Rat Plasma	Rat bile	Dog Plasma	Dog Bile	Dog Urine	Dog Feces
M1	Hydroxy + sulfate	554	257, **337**, 443, 464	188, 257	+	+	-	+	-	-
M2	N-dealkylation product (amine)	364	**241**, 347	172, 221	+	+	-	-	-	-
M3	Acylglucuronide of parent	624	**241**, 347	172, 221	-	+	-	-	-	-
M4	*N*-oxide #1	464	**241**, 347	172, 221	+	+	+	+	+	-
M5	Taurine conjugate	555	**241**, 347, 449	172, 221	+	+	-	-	-	-
M6	*N*-oxide #2	464	**241**, 347	172, 221	-	-	+	+	+	-
M7	Glutathione adduct	654	**241**, 347, 525, 579	172, 221	-	+	-	-	-	-
M8	Acylglucuronide of deamination product	554[d]	333, **377**	227, 333	-	+	-	+	-	-
M9	Lactam glucuronide	638	241, **442**, 462	296, 316	-	+	-	-	-	-
M10	N-dealkylation product (acid)	378[d]	**333**	227	-	-	+	+	-	+
M11	Lactam	462	241, **442**	no signal	+	+	-	-	-	-
S	MRL-A	448	**241**, 347	172, 221	+	+	+	+	+	+

[a] CID spectra of the metabolites were obtained in a data-dependent and list-dependent mode with the ion trap mass spectrometer in positive ionspray mode, except as indicated.

[b] MS2 indicates the marker ions in the product ion scan used for identification of the metabolite following CID of the molecular ion. The most predominant ion is bolded and underlined.

[c] MS3 indicates the ions formed following CID of the predominant product ion detected in MS2.

[d] metabolite detected under negative ionspray conditions.

DMD Fast Forward. Published on May 12, 2006 as DOI: 10.1124/dmd.105.009027

Figure 1

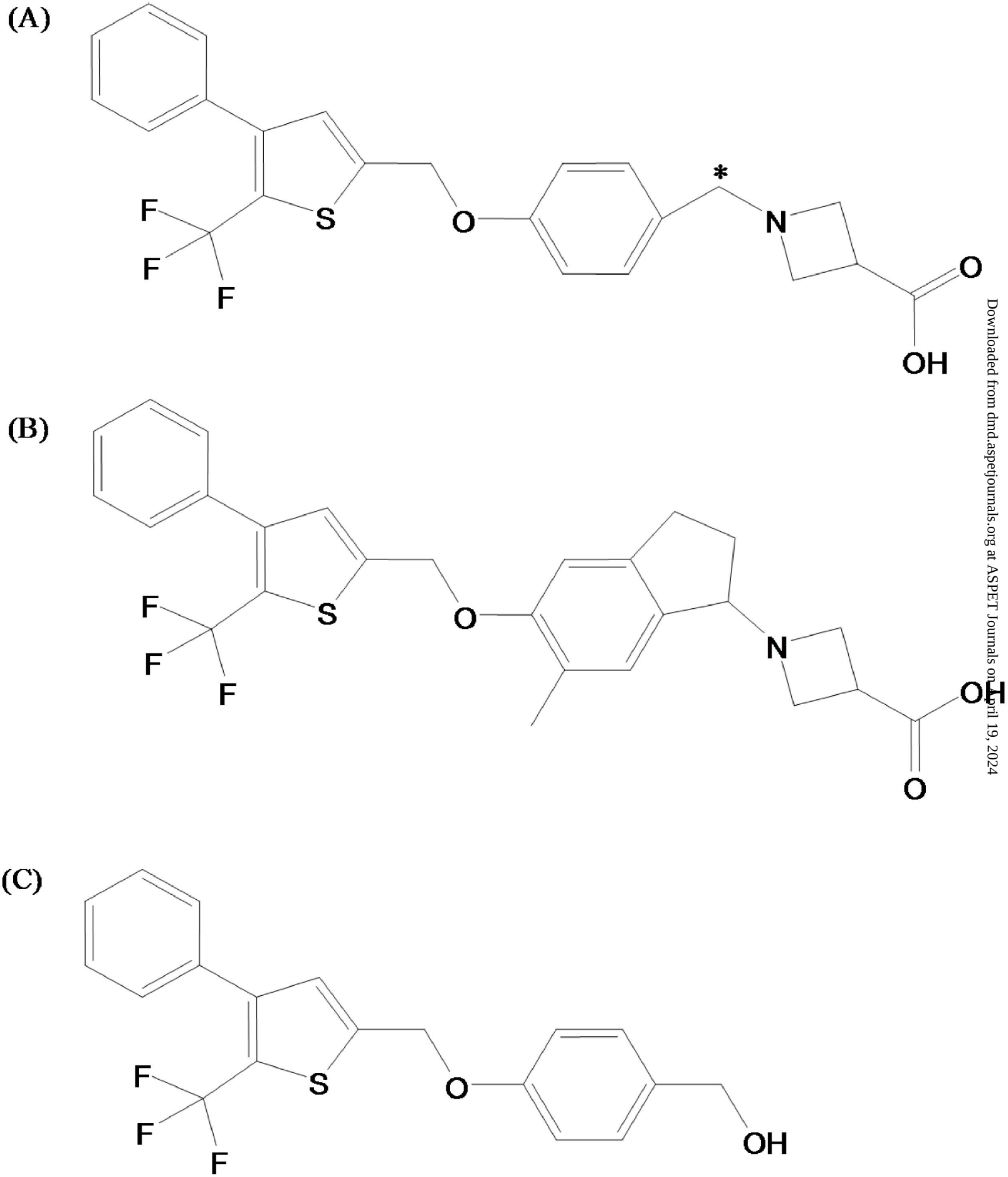

DMD Fast Forward. Published on May 12, 2006 as DOI: 10.1124/dmd.105.009027

Figure 2

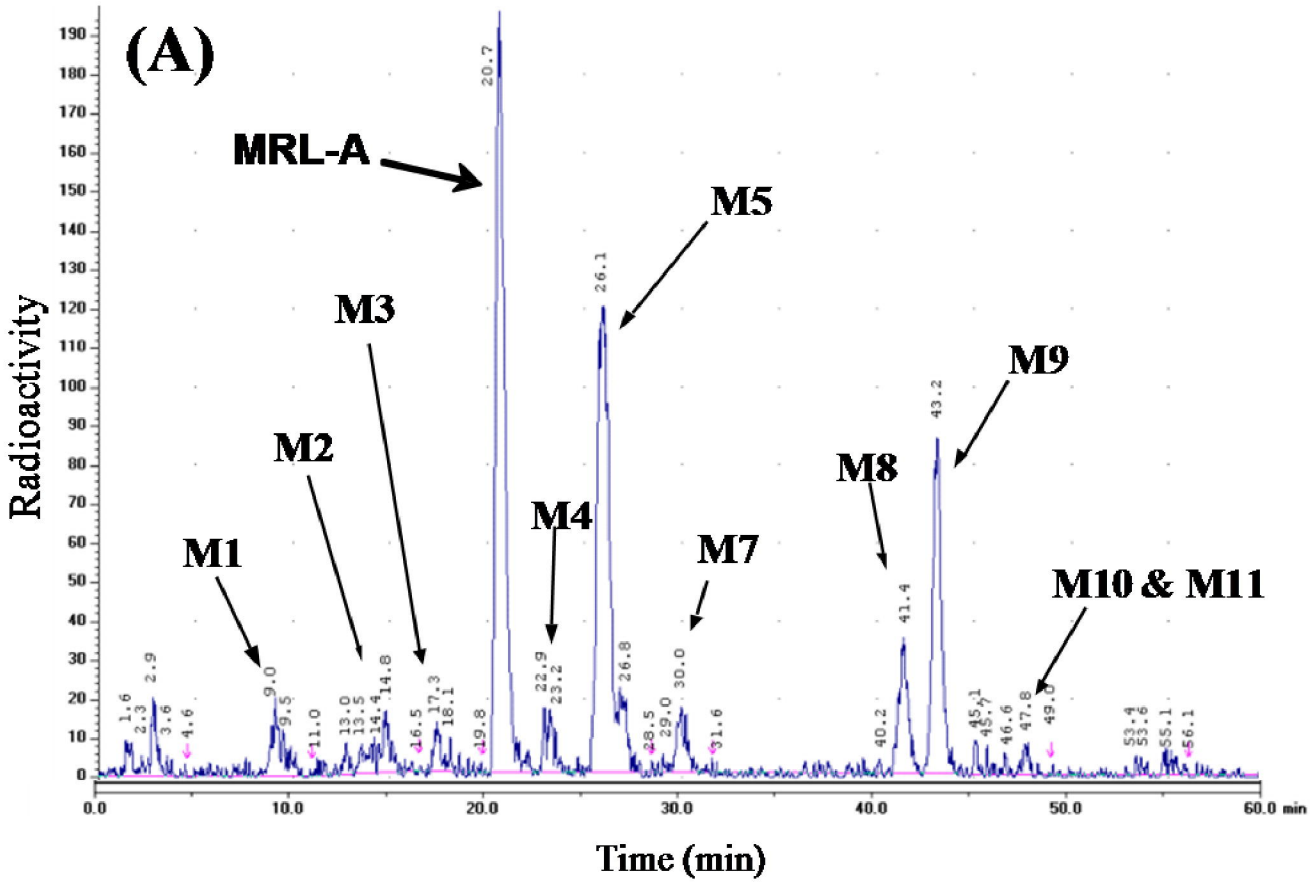

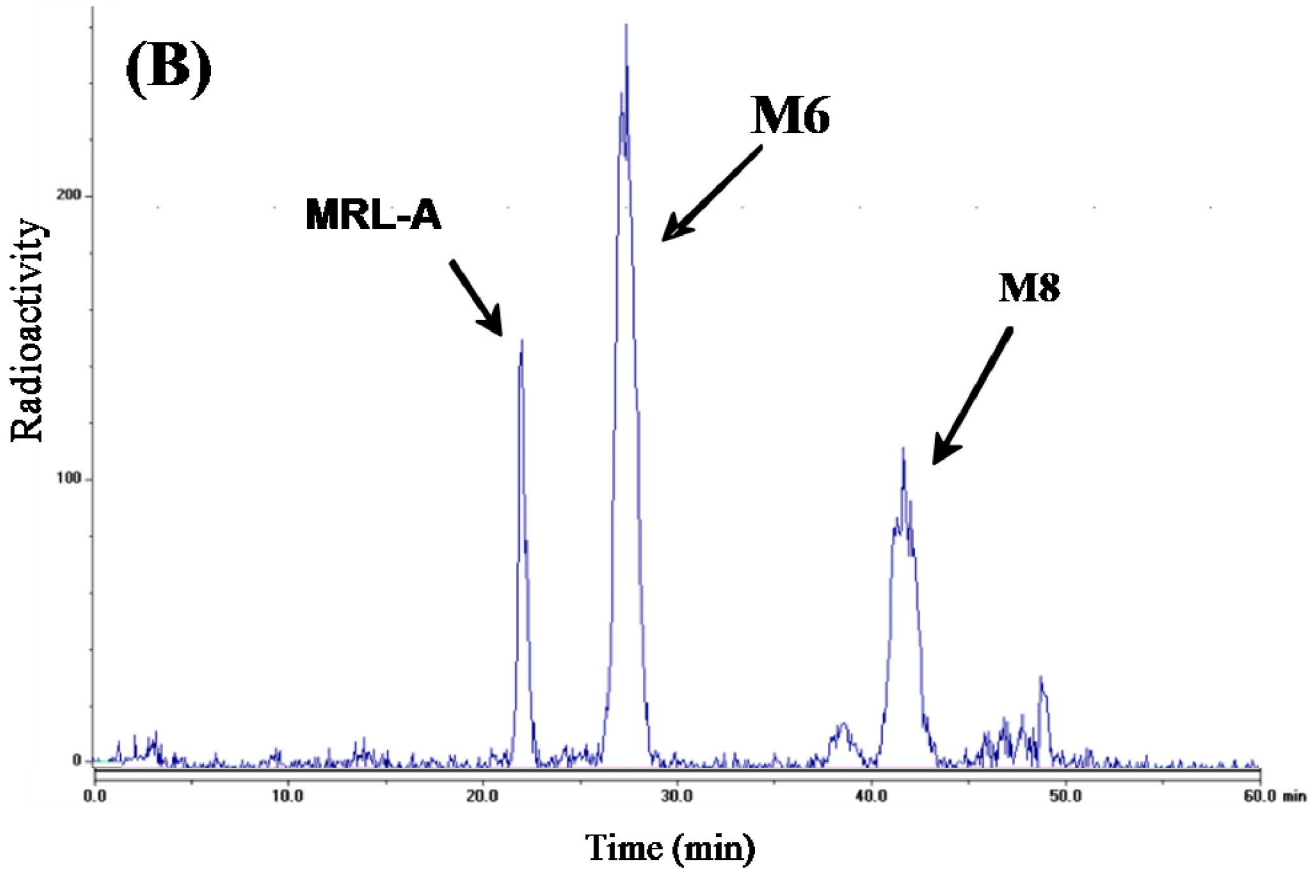

DMD Fast Forward. Published on May 12, 2006 as DOI: 10.1124/dmd.105.009027
This article has not been copyedited and formatted. The final version may differ from this version.

Figure 3

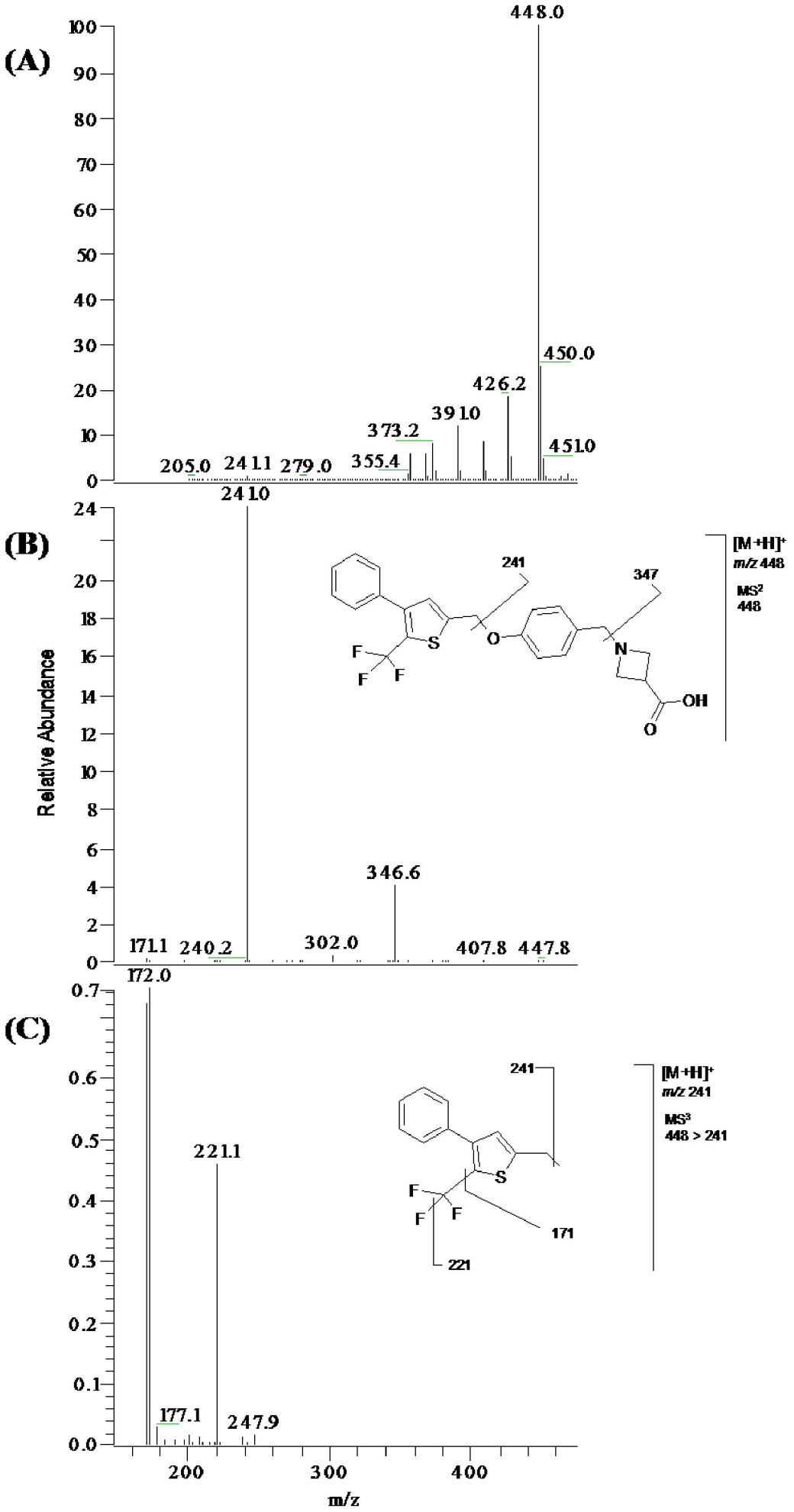

DMD Fast Forward. Published on May 12, 2006 as DOI: 10.1124/dmd.105.009027
This article has not been copyedited and formatted. The final version may differ from this version.

Figure 4

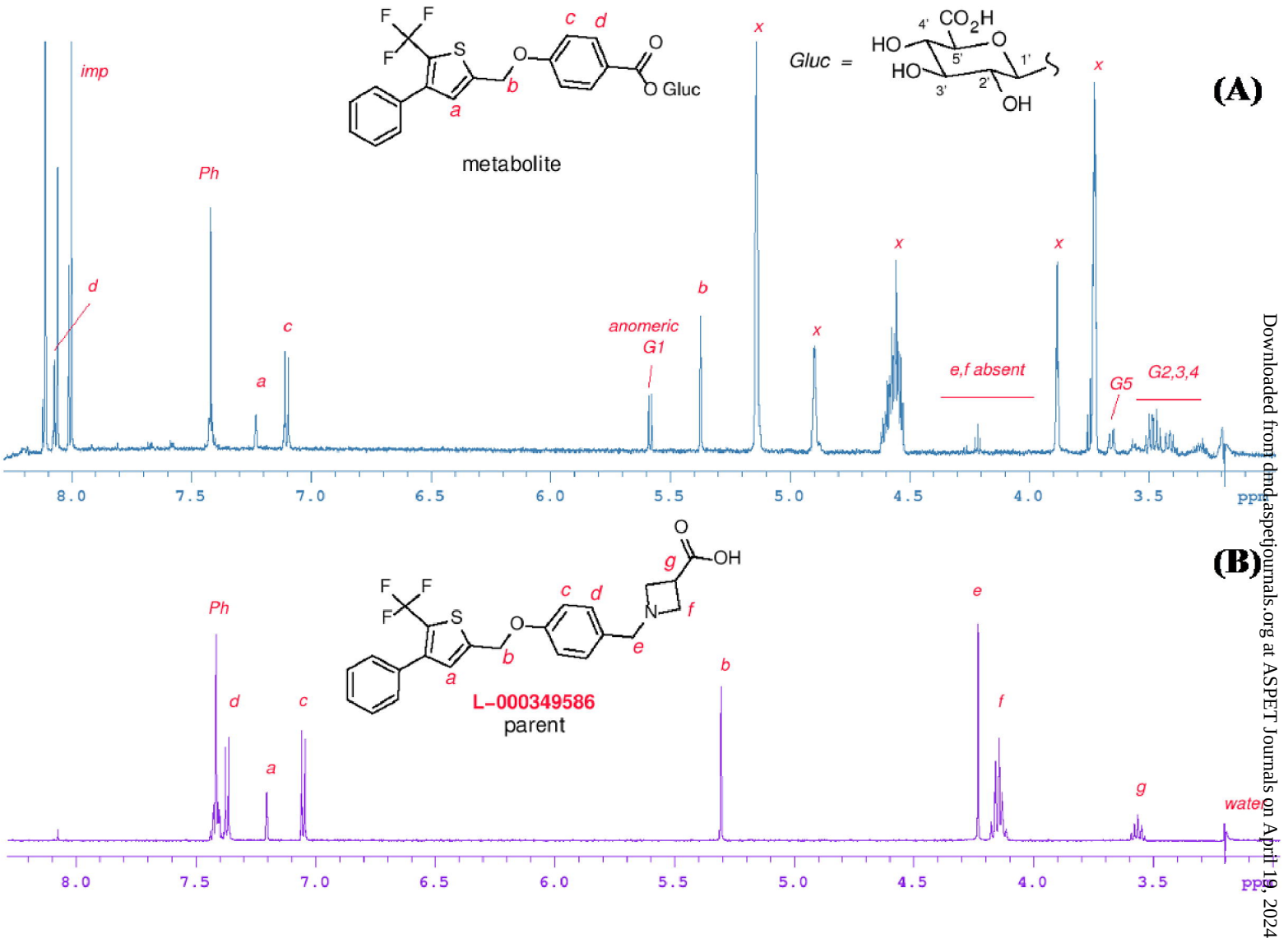

DMD Fast Forward. Published on May 12, 2006 as DOI: 10.1124/dmd.105.009027
This article has not been copyedited and formatted. The final version may differ from this version.

Figure 5

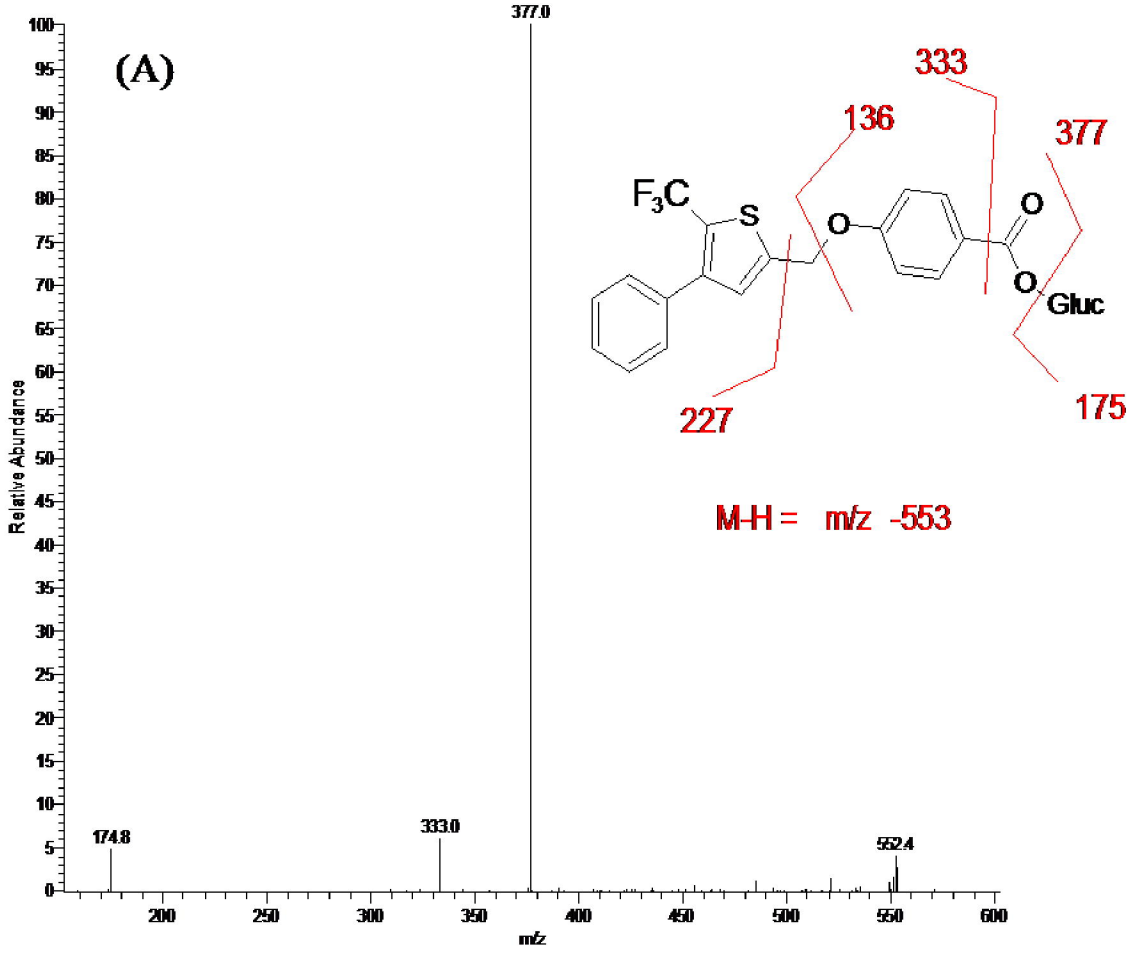

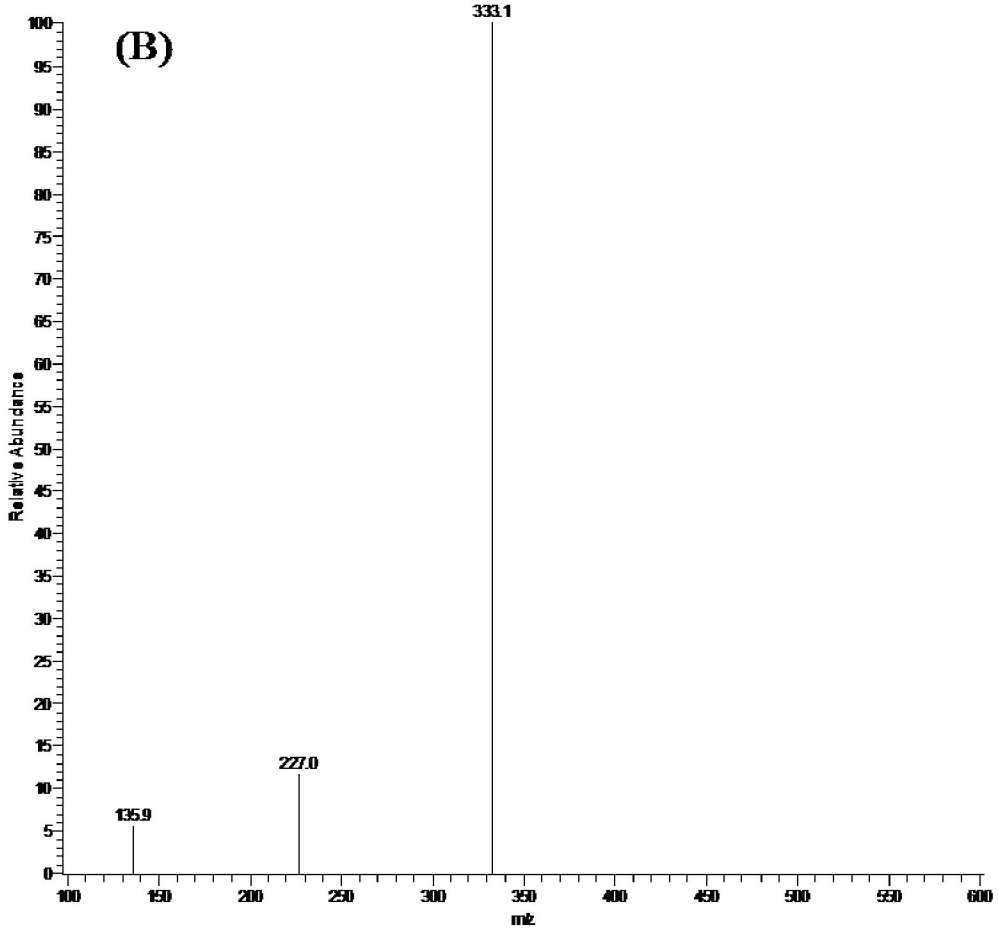

DMD Fast Forward. Published on May 13, 2005 as DOI: 10.1124/dmd.105.009027
This article has not been copyedited and formatted. The final version may differ from this version.

Figure 6

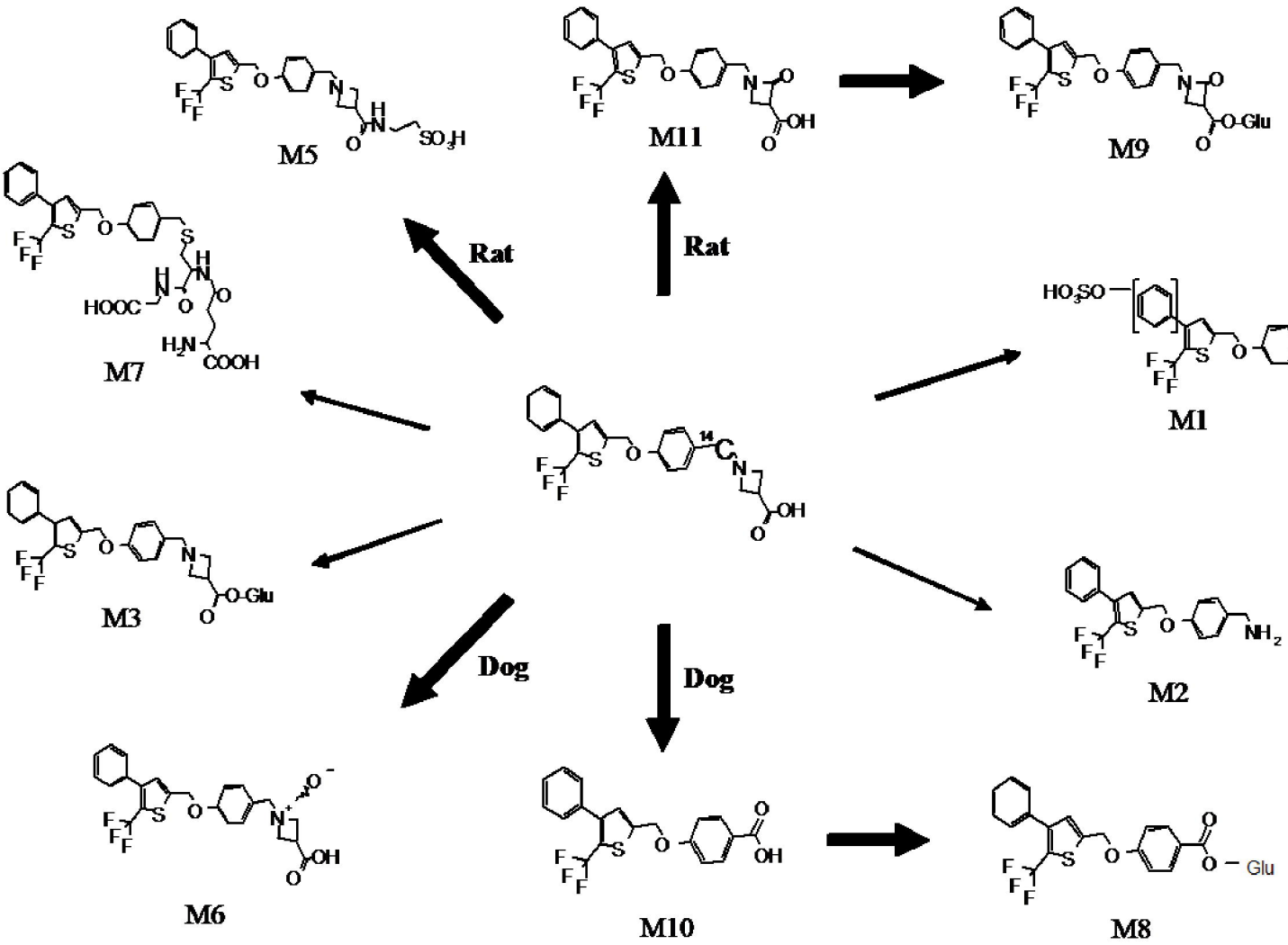

DMD Fast Forward. Published on May 12, 2006 as DOI: 10.1124/dmd.105.009027

Figure 7